Characteristics of tongue-shaped deformations in hydrogen and deuterium plasmas in the Large Helical Device

Characteristics of tongue-shaped deformations in hydrogen and deuterium plasmas in the Large Helical Device

S. Voermans,[1] K. Ida,[2, 3] T. Kobayashi,[2] M. Yoshinuma,[2] H. Tsuchiya,[2] T. Akiyama,[2] and M. Emoto[2]

[1]*Eindhoven University of Technology, Eindhoven, 5600 MB, The Netherlands*
[2]*National Institute for Fusion Science, National Institutes of Natural Sciences, Toki, Gifu 509-5292, Japan*
[3]*SOKENDAI (The Graduate University for Advanced Studies), Toki, Gifu 509-5292, Japan*
(Dated: July 15, 2019)

The tongue-shaped deformation (TSD), a possible trigger for the evolution of quasi-stable magneto hydrodynamic (MHD) modes into MHD bursts, was first experimentally identified in the Large Helical Device (LHD)[1]. Further analysis has been based on the experimental data in low density ($< 1.2 \times 10^{19} \text{m}^{-3}$) and low β (0.4%) hydrogen plasmas[2][3]. However, since the mechanism causing the tongue-shaped deformation has not been clarified, it is important to study the characteristics of this nonlinear instability in a more broad spectrum of experiments to stimulate the study in simulation and theory for this event. Identification of tongue-shaped deformations in both hydrogen and deuterium plasmas is automatised and characterization of the TSDs is done by quantifying their size, timing and location using ECE, RF and magnetic probe diagnostics. The dependence of these characteristics on plasma parameters such as density, toroidal rotation and NBI power is given.

I. INTRODUCTION

In helical plasmas various magneto hydrodynamic (MHD) modes are present and are found to be correlated to abrupt collapse events, threatening the stability of the plasma. One such mode is the energetic ion driven resistive interchange (EIC) mode, a rotating bursting $m/n = 1/1$ tearing parity mode, which resonates with the precession motion of helically-trapped energetic ions (EPs). In the Large Helical Device (LHD), these MHD bursts are often preceded by a quasi-stable stationary $m/n = 1/1$ interchange parity mode. During the evolution from this stationary MHD mode to the bursting mode the tongue-shaped deformation (TSD) is found. The TSD is a displacement of the equi-temperature surface at a non-rational magnetic flux surface, which enables magnetic field reconnection and parity change. It was first predicted by L.A. Artsimovich[4] and first observed during high ion-temperature shots in the Large Helical Device[1]. More extensive papers by K. Ida describe the distorted velocity distribution of epithermal ions due to the TSD and its evolution in time[2, 3]. The most likely cause of the destabilisation of the stationary MHD mode and the growth of the TSD and EIC mode is identified to be the presence of a high density of trapped energetic ions due to neutral beam injection (NBI)[5]. After the destabilisation expulsion of helically-trapped energetic ions is observed[6], which results in a decrease of NBI heating efficiency, quenched fusion burn and possible damage to plasma facing components[7, 8].

Since the mechanism causing the tongue-shaped deformation has not been clarified, and no analytical theory or model exist to predict or suppress the deformation, a study of the characteristics of the TSD from experimental data is performed. This to ensure experimental understanding of the event and stimulate the study of the TSD event in the field of simulation and theory. This study uses an extensive data pool of 200 experimental shots of the LHD, to determine the characteristics of the TSD in hydrogen and deuterium plasmas. The tongue-shaped deformation previously observed does not appear at low-order rational surface and does not oscillate for a long period (usually only one cycle sometimes a few cycle), which is different from a usual MHD mode. These characteristics suggest the tongue-shaped deformation is the result of a highly nonlinear instability and the size, timing and location of its appearance vary event by event. The TSD is toroidally and poloidally localised and has no helical structure expressed by toroidal and poloidal mode number, similar to finger-like ELM structures[9, 10] and solitary perturbations[11]. In this paper, the statistical analysis of size, timing and location of the tongue-shaped deformation is performed and the analysis method to quantify these characteristics is given in the following section. Then the results of the statistical analysis are shown. In the next section, the dependency of the characteristics on plasma parameters including density, toroidal rotation, and power deposited by NBIs are given. The results are summarised in the last section.

II. METHOD

The standard configuration of the Heliotron-type Large Helical Device has a magnetic field, B, of $2.75 - 2.85$T, a major radius, R_{ax}, of 3.6m and an effective minor radius, r_{eff}, of 0.65m. In this paper, the effective minor radius is normalised by a_{99}, the radius at which 99% of the plasma current is encircled. a_{99} depends on plasma parameters but is close to 0.64m. The plasma electron density, n_e, in the shots analysed ranges between $0.8 - 1.6 \times 10^{-19} \text{m}^{-3}$ and the ion temperature, T_i, ranges between $2 - 7$keV. The device has three tangential ports for neutral beam injection (NBI), one CW and two CCW, and two ports for perpendicular NBIs. The injection energy of the tangential beams is $160 - 180$keV and the injection power totals

16MW. The energy of the two perpendicular beams is lower at $40-50$keV with an injection power of 12MW[12]. A typical TSD event in a hydrogen plasma with electron density $n_e \approx 1 \times 10^{-19}$m^{-3} and central ion temperature $T_i \approx 3.5$keV is shown in figure 1.
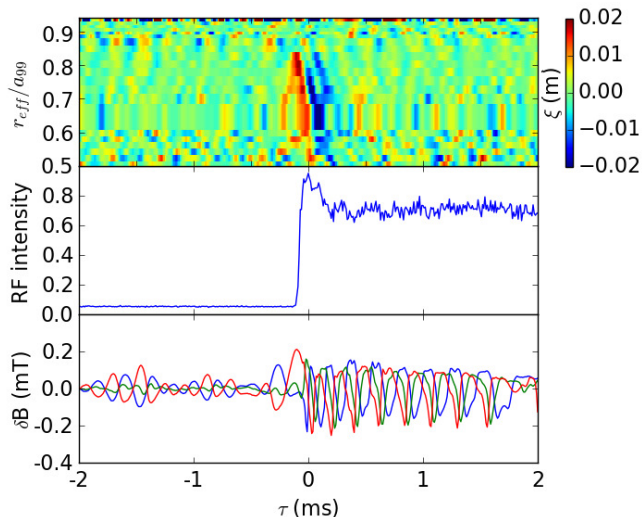
Figure 1: The tongue-shaped deformation in hydrogen shot 116190 and its accompanying peak in RF signal and magnetic field perturbation at toroidal angles of 90° (blue), 198° (green) and 270° (red).

The first plot depicts the displacement of the plasma, ξ, with respect to the relative time, τ, and the normalised effective radius r_{eff}/a_{99}. The displacement is defined as $\xi = \frac{\delta T_e}{\nabla T_e}$, where the the high frequency $(1 - 10\mathrm{kHz})$ change in electron temperature, δT_e, and the low frequency $(40\mathrm{Hz})$ gradient in the temperature, ∇T_e, are measured with electron cyclotron emission (ECE) diagnostics and are passed through high pass and low pass filters respectively[13, 14]. A positive value of the displacement is equal to an outward shift of the plasma while a negative value is equal to an inward shift.

Peak values of the normalised output of the high frequency RF probe of 880MHz are used as a trigger of the timing of the tongue event, as peaked high frequency radiation indicates loss of energetic ions at the plasma edge[15, 16]. The start of relative time, $\tau = 0$ms, is set to the moment of the RF peaks attain their highest value. The peak in the RF signal for the described TSD is shown in the second plot of figure 1.

The last plot shows the perturbation of the magnetic field, δB measured by magnetic probes at toroidal angles of 90° (blue), 198° (green) and 270° (red)[17]. From this perturbation the transition from a quasi-stable stationary MHD to a bursting rotating MHD mode can be seen. Before the peak in RF signal intensity it shows an out-of-phase relation between probe signals from toroidal angles of 90° and 270°, while the probe of 198° has a small amplitude, indicating a non-rotating standing wave MHD mode. Just before and during the peak in RF signal the

amplitude of the 270° probe signal increases dramatically, while the other stay approximately equal, indicating a localised deformation. After the RF signal peak the amplitude of all three signals are similar and the phase shift between them is constant, showing a toroidally rotating mode.

In figure 2, the same information is shown for a typical TSD event in a deuterium plasma with electron density $n_e \approx 1.1 \times 10^{-19}$m^{-3} and central ion temperature, $T_i \approx 3.7$keV. It can be seen that, while at first the frequency of the rotating MHD mode is higher, the TSD, RF and magnetic probe signals are quite similar to that of the event in hydrogen.
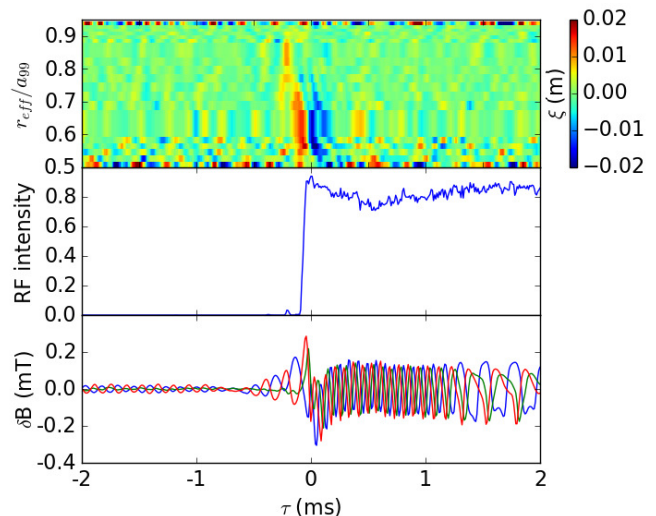
Figure 2: The tongue-shaped deformation in deuterium shot 150088 and its accompanying peak in RF signal and magnetic field perturbation at toroidal angles of 90° (blue), 198° (green) and 270° (red).

To characterise the TSD events methodically, two points in the development of the TSD event are of importance, the start and the maximum value of the displacement. The statistics on the timing and position of the start of the TSD give insight in the location of possible seed instability in time and space. Including the timing and position of the maximum value gives knowledge about the propagation of the TSD in space. The timing and radial location of the start of the events are parameterised by τ_{start} and $r_{\mathrm{eeff}}^{\mathrm{start}}/a_{99}$. These values obtained by searching for the earliest displacement in a time window of $\tau = \pm 0.3$ms around $\tau = 0$ms which satisfies $\xi \geq 3\sigma$, where σ is the standard deviation of ξ determined by analysing data between $\tau = -4$ms and $\tau = -0.3$ms. The value, ξ_{max}, the relative time, τ_{max}, and the radial position, $r_{\mathrm{eff}}^{\mathrm{max}}/a_{99}$, of the positive maximum of ξ are sought after in a time window of $\tau = \pm 0.25$ms around $\tau = 0$ms. Figure 3 shows the same event as figure 1, but now the locations of the maximum displacement during the event, m, and the start of the deformation, s, can be seen in the contour plot and their respective time slices of $r_{\mathrm{eff}}/a_{99} =$

0.81 and 0.65. Also shown in this figure is the time slice of $r_{\text{eff}}/a_{99} = 0.89$, which shows high amount of noise. This time slice is included to show that for channels with high amount of noise in the 3σ threshold is high enough to prevent possible wrong allocation of the start of the displacement.
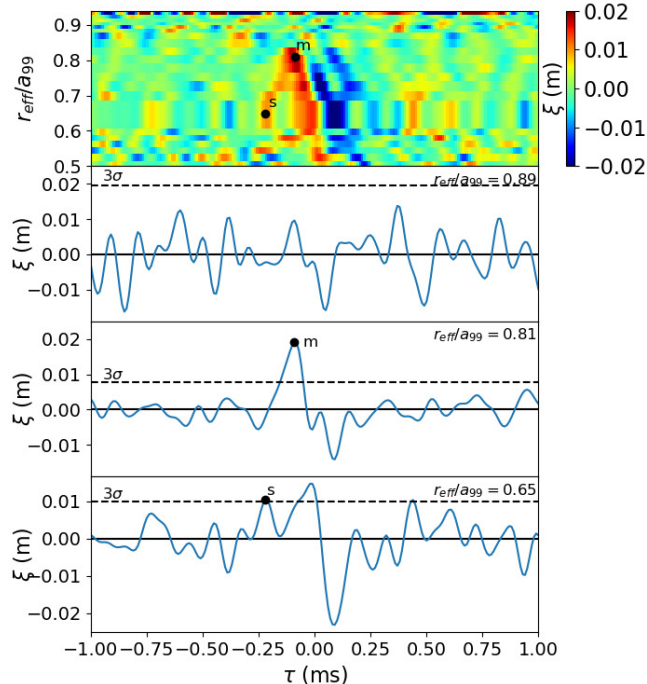
Figure 3: Contour plot and time slices of the tongue-shaped deformation in hydrogen shot 116190. The time slices show the deformation at positions of $r_{\text{eff}}/a_{99} = 0.89, 0.81$ and 0.65 which respectively show a channel with high amount of noise, the channel which contains the maximum value of the event and the channel which contains the starting position of the deformation. The dashed lines indicate the 3σ threshold and the black dots indicate the position of the start, s, and the maximum deformation, m, of the event.

III. STATISTICAL ANALYSIS

A total 200 of shots with varying parameters are analysed in this paper. In 98 shots at least one tongue-shaped deformation is found, 40 of these shots take place in a pure hydrogen plasma while the other 58 take place in a mixture of hydrogen and deuterium, for ease called 'deuterium plasmas'. Figures 4 and 5 show the statistics of the start of the TSD events in hydrogen plasmas and deuterium plasmas, respectively. The start of the deformation is generally located between -0.3ms and -0.2ms for both the hydrogen and deuterium shots. The preferred position of the start of the deformation is peaked around $r_{\text{eff}}/a_{99} = 0.81$ for the hydrogen shots, while the deuterium shots show a more divided profile with a high amount of counts around $r_{\text{eff}}/a_{99} = 0.81$, but also around

$r_{\text{eff}}/a_{99} = 0.70$. The black lines plotted in the figures show the rational surfaces linked to the inverse of the vacuum rotational transform, $2\pi/\iota = m/n = 2/1, 3/2, 4/3$ and $1/1$, located at $r_{\text{eff}}/a_{99} = 0.5443, 0.7239, 0.7714$ and 0.9192 respectively. Unfortunately, the positions of these rational surfaces can deviate from the given vacuum profile values due to plasma currents. However, during these measurements relatively low (20kA) plasma currents develop and high (2.8T) magnetic fields are present, and the deviation is predicted to be less than 1% of the minor radius[18]. It should be noted that there is almost no tongue-shaped deformation staring at the low-order rational surfaces, where the usual oscillating MHD instability appears. As the surfaces of $m/n = 3/2$ and $m/n = 4/3$ lie quite close to the preferred position, it is possible that seed instabilities from these rational surfaces grow non-linearly into the TSD events, however the provided data cannot prove this, thus further theoretical analyses should be performed to investigate the growth from seed instability to TSD.
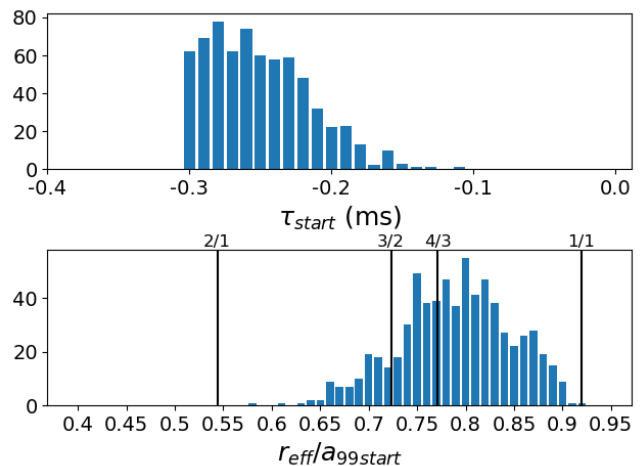
Figure 4: Histograms showing the timing and position of the start of the TSD events in hydrogen plasmas. The histogram with respect to position also shows the location of rational surfaces $2\pi/\iota = m/n$ represented by the black lines.

The statistics of the maximum of the displacement in hydrogen plasmas can be seen in figure 6. This figure shows three histograms with respect to the maximum size of the displacement ξ_{max}, the position of the maximum, $r_{\text{eff}}^{\text{max}}/a_{99}$, and the relative time, τ_{max} for 1060 TSD events in the 40 hydrogen plasma shots. It is clearly seen that TSD events generally result in maximum deformations between $1-2$cm. The most probable radial position to find the maximum deformation is peaked at two values, $r_{\text{eff}}^{\text{max}}/a_{99} = 0.65$ and $r_{\text{eff}}^{\text{max}}/a_{99} = 0.81$. This indicates that the evolution from start to maximum can go in two different ways: either the TSD grows larger at the radial position where it starts around $r_{\text{eff}}/a_{99} = 0.81$ until its maximum value has been reached, or it propagates inwards from its starting position to a position around $r_{\text{eff}}^{\text{max}}/a_{99} = 0.65$. These propagation paths are correlated

4
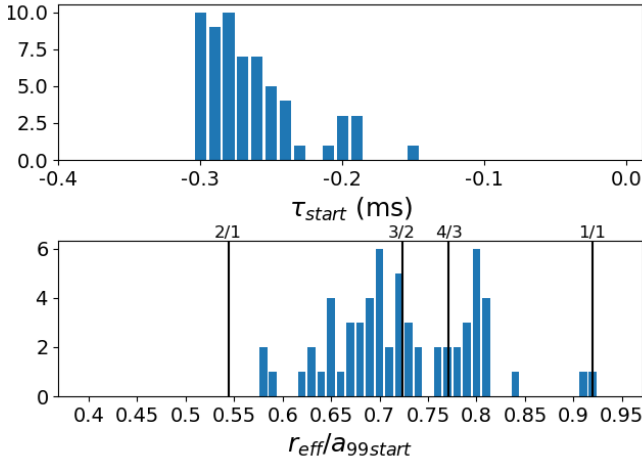
Figure 5: Histograms showing the timing and position of the start of the TSD events in deuterium plasmas. The histogram with respect to position also shows the location of rational surfaces $2\pi/\iota = m/n$ represented by the black lines.

Figure 6: Histograms of the amount of TSD events as a function of maximum displacement, location and timing in hydrogen plasmas.

Figure 7: Histograms of the amount of TSD events as a function of maximum displacement, location and timing in deuterium plasmas.

to the timing of the maxima, as can be seen from the colouring in figure 6. The shots which attain their maximum around $r_{\mathrm{eff}}/a_{99} = 0.81$ are coloured orange, and in the histogram with respect to relative time these shots are found to be located mostly between $\tau_{\mathrm{max}} = -0.2\mathrm{ms}$ and $\tau_{\mathrm{max}} = -0.1\mathrm{ms}$, while the blue coloured shots, which attain their maximum around $r_{\mathrm{eff}}^{\mathrm{max}}/a_{99} = 0.65$, are located between $\tau_{\mathrm{max}} = -0.1\mathrm{ms}$ and $\tau_{\mathrm{max}} = 0\mathrm{ms}$. This proves that the TSDs which grow larger at the place of their appearance in the manner described first, obtain their maximum earlier than the TSD events which propagate inward towards their maximum. In black the positions of the rational surfaces are given again. It can be seen that the most probable maximum position is, just like the most probable start position, not located at rational surfaces of $m/n = 1/1$ or $m/n = 1/2$. However, the distinct separation between two preferred positions may suggest some interaction between the TSD, which grows non-linearly, and the linear MHD instability existing at the two rational surfaces $m/n = 3/2$ and $m/n = 4/3$. The theoretical study of the interaction between non-linear and linear instability is advised for future work. As a last conclusion from this figure, the histogram as a function of relative time shows that the majority of τ_{max} is smaller than $\tau = 0\mathrm{ms}$, indicating that the TSDs happen before, and therefore are the cause and not the result of, the RF peaks and the loss of energetic ions.

In figure 7 the same histograms are shown but now count the 190 TSD events in the 58 deuterium plasma shots. TSD events are thus clearly less prominent in deuterium plasmas than in hydrogen plasmas. The values of the maximum displacement show a very similar distribution to that of hydrogen, as it also ranges between $1 - 2\mathrm{cm}$. However, the statistics of TSDs in deuterium plasmas as a function of position and time are not similar to their respective statistics in hydrogen plasmas, as there is no
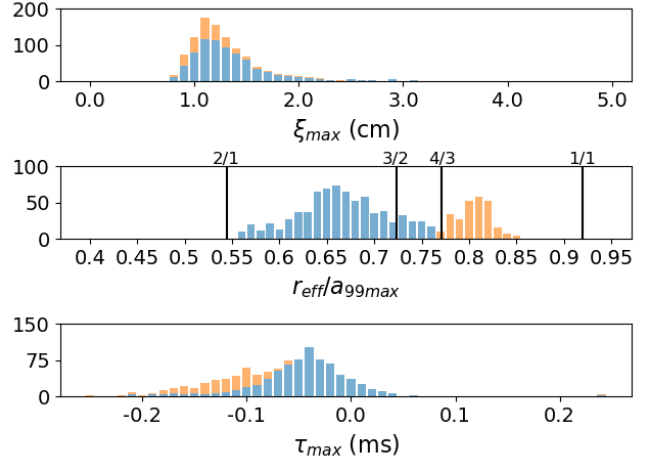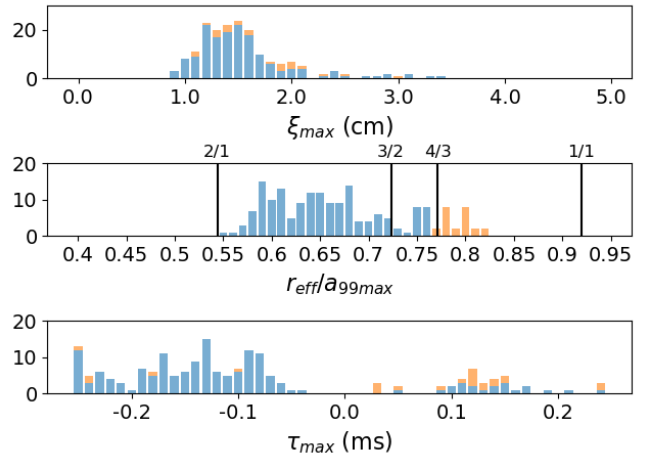
clear second peak in the histogram with respect to position, no clear correlation between the position and timing of counts around $r_{\mathrm{eff}}^{\mathrm{max}}/a_{99} = 0.81$ indicated in orange, and there are now a noticeable amount of counts around $\tau_{\mathrm{max}} = 0.12\mathrm{ms}$. The first and second observations indicate that the second method of propagation, where the TSD starts at a relative outward position and propagates inwards, is most dominant in deuterium plasmas. The unexpected amount of counts at $\tau_{\mathrm{max}} > 0$ can be explained by looking at figure 8. Here, the behaviour of the displacement event differs from the standard behaviour, as not only one cycle of outward and inward displacement can be seen in time, but multiple cycles. RF intensity due to this event is low with respect to the normal TSD event, and alternating positive and negative magnetic perturbation copies the outward and inward displacement seen in

the ECE data, preventing it from showing the expected behaviour of the bursting MHD mode. This multi-cycle tongue-shaped deformation behaviour is encountered in 50 of the 190 TSD events in the deuterium shots. For 40 of the multi-cycle TSDs the maximum value of the whole event is located in the outward displacement of the plasma in the second cycle rather than in the first. These 40 TSD events have a τ_{max} which is approximately 0.3ms, the length of one period of the cycle, later than the expected timing between $\tau = -0.1$ms and $\tau = -0.2$ms. Multiple cycles of the TSD indicate that the free energy in the instability is not exhausted during the first outward displacement, such that a second or even third displacement has to follow.
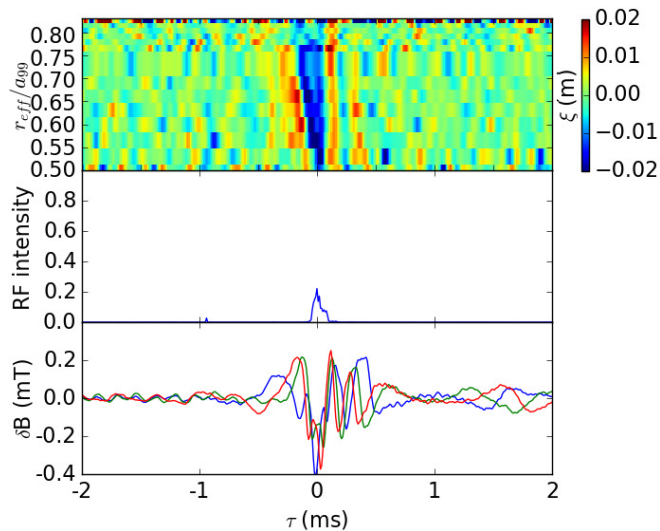
Figure 8: The tongue-shaped deformation, RF intensity and magnetic perturbation at toroidal angles of 90° (blue), 198° (green) and 270° (red) in shot 145051, which shows a multi-cycle event.

IV. DEPENDENCY

The dependence of the TSD on electron density, toroidal rotation, and NBI power is discussed here. The electron density is likely to influence the presence of tongue-shaped deformations in the plasma. A high electron density will result in a short slowing down time of the helically-trapped energetic ions, decreasing the population density and, as the evolution of the non rotating m/n=1/1 mode into the growing tongue-shaped deformation is a process dependent on this density, have an effect on the formation of tongue-shaped deformations. This effect is shown in figure 9, where a series of seven hydrogen plasma shots is depicted in a histogram. The shots are performed with almost equal temperature profiles and NBI heating settings, but their electron density is varied. In this histogram a clear trend can be seen where TSD events in shots with higher density have lower maximum

displacement values. This trend shows that high electron density inhibits the formation of the tongue-shaped deformation.
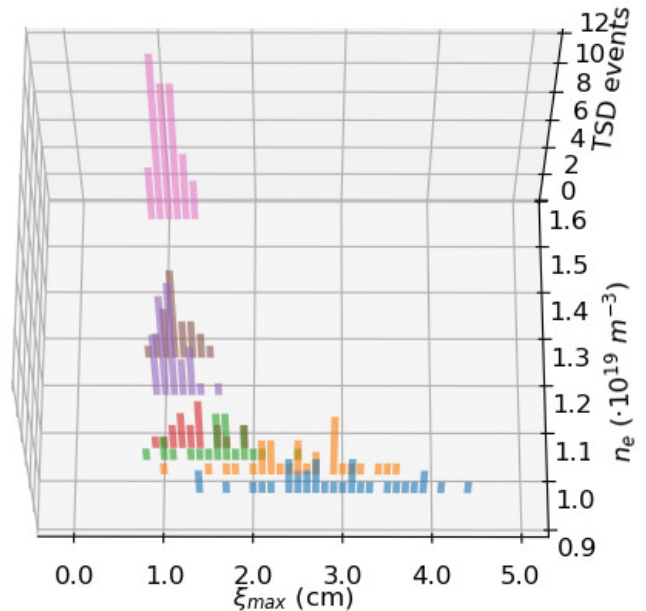
Figure 9: Histogram of the maximum displacement during the TSD events, ξ_{max}, with respect to seven hydrogen plasma shots of increasing electron density.

The toroidal rotation velocity of the plasma is also analysed as rotation in the plasma breaks the localisation of the high density of helically-trapped energetic ions. The deposition position of the NBIs is fixed in space and thus locally increases the trapped ion population. If the plasma rotates at high velocity, the trapped ion density will not reach a high value at a localised position. Higher toroidal rotation would thus mean a lower amount of TSDs which depend on this high density. In figure 10 the toroidal velocity, V_t, and the intensity of the RF signal are shown during a plasma shot in hydrogen where the density is almost constant at $n_e = 1.4 \times 10^{19}$m^{-3}. This figure shows an example of the behaviour of TSD event formation which is seen in many shots, in which a higher toroidal rotation results in fewer TSD events and thus fewer RF peaks. For this shot the distinction can be made between the period before and after $t = 4.8$s, where the toroidal rotation drops below ≈ 50km/s and the frequency of RF peaks increases.

As the TSD growth depends on the density of energetic particles, increasing this density is expected to increase the amount of events seen in a particular shot. An increased value of the power of NBIs will result in such an increase of the helically-trapped energetic particles in the plasma, as it introduces more high velocity particles which get ionised. However, the NBI power is coupled to the plasma rotation, as the higher power of tangential NBIs introduces more energetic particles with a velocity in the direction of that particular NBI beam, resulting in
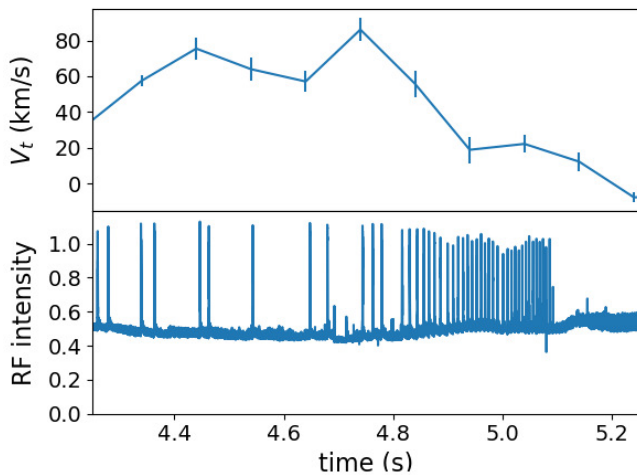
Figure 10: Toroidal velocity, V_t and intensity of the RF probe signal during shot 116163 in a hydrogen plasma.

rotation of the plasma. In LHD, tangential NBI beams 1 and 3 are pointed in the opposite direction to NBI beam 2. Figure 11 shows the histogram for shots with increasing effective NBI 1 and NBI 3 power, calculated by multiplying the power by the time each of the NBIs is active, and increasing toroidal rotation velocity, V_ϕ. The density and ion temperature are kept approximately constant in the included shots at a value of $n_e \approx 1.3 \times 10^{19} \mathrm{m}^{-3}$ and $T_i \approx 5\mathrm{keV}$ respectively and the power of NBI beams 2, 4 and 5 are also kept constant.
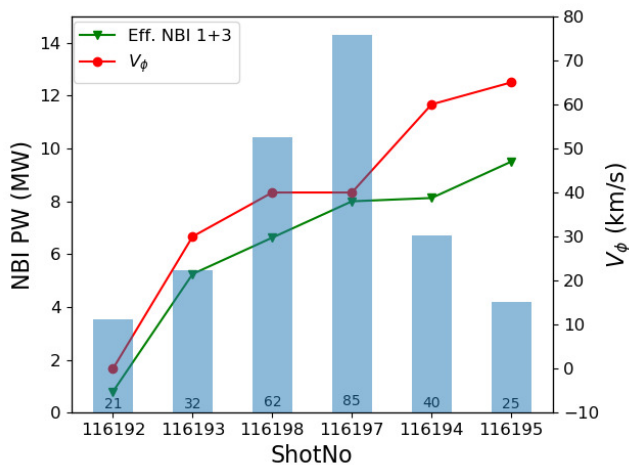
Figure 11: Histogram of the amount of TSD events per plasma shot with respect to increasing NBI power and toroidal rotation velocity.

A clear optimum can be seen where neither the NBI power nor the toroidal velocity is maximum. The figure shows that increasing NBI power is positive for the emergence of TSD events, as expected. However, high toroidal rotation will prevent the buildup of the trapped ion population and thus prevent the growth of tongue-shaped

deformations, decreasing the amount of events seen in the last two shots.

V. SUMMARY

The most striking finding of this study on the characteristics of the tongue-shaped deformation is that the start location has a very wide spectrum and tongue-shaped deformation always starts between, not at, the two locations of low-order rational surface $m/n = 1/2$ and $m/n = 1/1$. An other interesting finding is that maximum displacement generally appears not at a single, but at either of two distinct non-rational surfaces in hydrogen plasmas, $r_{\mathrm{eff}}/a_{99} = 0.65$ and $r_{\mathrm{eff}}/a_{99} = 0.81$. The two peaks of the most probable maximum displacement location suggest the possibility of interaction of TSDs with linear MHD instability existing at the rational surface of $m/n = 3/2$ and $m/n = 4/3$. A clear difference between the behaviour of tongue-shaped deformations in hydrogen and deuterium plasmas has been seen, the TSD events are more prominent in hydrogen plasmas than in deuterium plasmas. This can be concluded from the fact that there are 1060 TSDs observed in 40 hydrogen shots, while only 190 TSDs are seen in 58 deuterium shots. Also, a new kind of behaviour of the TSD has been found in 50 of the deuterium plasma events: multiple cycles (2 or 3) of outward and inward plasma displacement. Dependence of the TSD showed as expected: a higher density reduces the maximum displacement during TSDs, a higher toroidal rotation reduces the amount of TSD events in a particular shot and more NBI power increases this amount. As a high amount of tongue-shaped deformations results in high loss of energetic particles, and therefore less effective NBI heating, quenched fusion burn and possible damage to plasma facing components, these conclusions should be taken into account when designing new experiments on the Large Helical Device.

[1] K Ida, T Kobayashi, K Itoh, M Yoshinuma, T Tokuzawa, T Akiyama, C Moon, H Tsuchiya, S Inagaki, and S-I Itoh. Abrupt onset of tongue deformation and phase space response of ions in magnetically-confined plasmas. *Scientific Reports*, 6:36217, 2016.

[2] K Ida, T Kobayashi, M Yoshinuma, T Akiyama, T Tokuzawa, H Tsuchiya, K Itoh, and LHD Experiment Group. Observation of distorted maxwell-boltzmann distribution of epithermal ions in lhd. *Physics of Plasmas*, 24(12):122502, 2017.

[3] K Ida, T Kobayashi, M Yoshinuma, T Akiyama, T Tokuzawa, H Tsuchiya, K Itoh, and S-I Itoh. Trigger mechanism for the abrupt loss of energetic ions in magnetically confined plasmas. *Scientific reports*, 8(1):2804, 2018.

[4] LA Artsimovich. *A Physicist's ABC on Plasma*. Moscow: Mir Publishers, 1978.

[5] XD Du, K Toi, S Ohdachi, M Osakabe, T Ido, K Tanaka, M Yokoyama, M Yoshinuma, K Ogawa, KY Watanabe, et al. Resistive interchange mode destabilized by helically trapped energetic ions and its effects on energetic ions and bulk plasma in a helical plasma. *Nuclear Fusion*, 56(1):016002, 2015.

[6] K Ogawa, M Isobe, H Kawase, T Nishitani, R Seki, M Osakabe, LHD Experiment Group, et al. Observation of enhanced radial transport of energetic ion due to energetic particle mode destabilized by helically-trapped energetic ion in the large helical device. *Nuclear Fusion*, 58(4):044001, 2018.

[7] Kunihiro Ogawa, Mitsutaka Isobe, and Kazuo Toi. Beam ion losses caused by magnetic field ripples in various plasma parameter ranges in the large helical device. *Plasma and Fusion Research*, 7, 2012.

[8] Kunihiro Ogawa, Mitsutaka Isobe, and Kazuo Toi. Design study of a lost fast-ion probe in large helical device. *Plasma and Fusion Research*, 3:S1082–S1082, 2008.

[9] GS Yun, Woochang Lee, MJ Choi, J Lee, HK Park, B Tobias, CW Domier, NC Luhmann Jr, AJH Donné, JH Lee, et al. Two-dimensional visualization of growth and burst of the edge-localized filaments in kstar h-mode plasmas. *Physical review letters*, 107(4):045004, 2011.

[10] GS Yun, W Lee, MJ Choi, J Lee, HK Park, CW Domier, NC Luhmann Jr, B Tobias, AJH Donné, JH Lee, et al. Two-dimensional imaging of edge-localized modes in kstar plasmas unperturbed and perturbed by n= 1 external magnetic fields. *Physics of Plasmas*, 19(5):056114, 2012.

[11] JE Lee, GS Yun, W Lee, MH Kim, M Choi, J Lee, M Kim, HK Park, JG Bak, WH Ko, et al. Solitary perturbations in the steep boundary of magnetized toroidal plasma. *Scientific reports*, 7:45075, 2017.

[12] Yasuhiko Takeiri, Osamu Kaneko, Masaki Osakabe, Kenichi Nagaoka, Sadayoshi Murakami, Hiromi Takahashi, Haruhisa Nakano, Katsumi Ida, Shigeru Morita, Masayuki Yokoyama, et al. Development of the heating scenarios to achieve high-ion temperature plasma in the large helical device. *Plasma and Fusion Research*, 10: 1402001–1402001, 2015.

[13] Y Nagayama, K Kawahata, A England, Y Ito, N Bretz, M McCarthy, G Taylor, J Doane, H Ikezi, T Edlington, et al. Electron cyclotron emission diagnostics on the large helical device. *Review of scientific instruments*, 70(1): 1021–1024, 1999.

[14] Hayato Tsuchiya, Yoshio Nagayama, Kazuo Kawahata, Shigeru Inagaki, Shin Kubo, LHD Experiment Group, et al. Design and installation of a new electron cyclotron emission diagnostic antenna in lhd. *Plasma and Fusion Research*, 6:2402114–2402114, 2011.

[15] Kenji Saito, Ryuhei Kumazawa, Tetsuo Seki, Hiroshi Kasahara, Goro Nomura, Fujio Shimpo, Hiroe Igami, Mitsutaka Isobe, Kunihiro Ogawa, Kazuo Toi, et al. Measurement of ion cyclotron emissions by using high-frequency magnetic probes in the lhd. *Plasma Science and Technology*, 15(3):209, 2013.

[16] KE Thome, DC Pace, RI Pinsker, O Meneghini, CA Del Castillo, and Y Zhu. Radio frequency measurements of energetic-particle-driven emission using the ion cyclotron emission diagnostic on the diii-d tokamak. *Review of Scientific Instruments*, 89(10):10I102, 2018.

[17] Satoru Sakakibara, H Yamada, and LHD Experiment Group. Magnetic measurements in lhd. *Fusion Science and Technology*, 58(1):471–481, 2010.

[18] K Ida, M Yoshinuma, C Suzuki, T Kobuchi, KY Watanabe, and LHD Experiment Group. Measurements of rotational transform with motional stark effect spectroscopy. *Fusion Science and Technology*, 58(1):383–393, 2010.